The *Haemophilus ducreyi* LspA1 Protein Inhibits Phagocytosis By Using a New Mechanism Involving Activation of C-Terminal Src Kinase

Dana A. Dodd,[a] Randall G. Worth,[b] Michael K. Rosen,[c,d] Sergio Grinstein,[e] Nicolai S. C. van Oers,[a,f,g] Eric J. Hansen[a]

Department of Microbiology, The University of Texas Southwestern Medical School, Dallas, Texas, USA[a]; Department of Medical Microbiology and Immunology, University of Toledo College of Medicine and Life Sciences, Toledo, Ohio, USA[b]; Department of Biophysics, The University of Texas Southwestern Medical School, Dallas, Texas, USA[c]; Howard Hughes Medical Institute, The University of Texas Southwestern Medical School, Dallas, Texas, USA[d]; Cell Biology Program, Hospital for Sick Children, Toronto, Ontario, Canada[e]; Departments of Immunology[f] and Pediatrics[g], The University of Texas Southwestern Medical School, Dallas, Texas, USA

ABSTRACT ***Haemophilus ducreyi* causes chancroid, a sexually transmitted infection. A primary means by which this pathogen causes disease involves eluding phagocytosis; however, the molecular basis for this escape mechanism has been poorly understood. Here, we report that the LspA virulence factors of *H. ducreyi* inhibit phagocytosis by stimulating the catalytic activity of C-terminal Src kinase (Csk), which itself inhibits Src family protein tyrosine kinases (SFKs) that promote phagocytosis. Inhibitory activity could be localized to a 37-kDa domain (designated YL2) of the 456-kDa LspA1 protein. The YL2 domain impaired ingestion of IgG-opsonized targets and decreased levels of active SFKs when expressed in mammalian cells. YL2 contains tyrosine residues in two EPIYG motifs that are phosphorylated in mammalian cells. These tyrosine residues were essential for YL2-based inhibition of phagocytosis. Csk was identified as the predominant mammalian protein interacting with YL2, and a dominant-negative Csk rescued phagocytosis in the presence of YL2. Purified Csk phosphorylated the tyrosines in the YL2 EPIYG motifs. Phosphorylated YL2 increased Csk catalytic activity, resulting in positive feedback, such that YL2 can be phosphorylated by the same kinase that it activates. Finally, we found that the *Helicobacter pylori* CagA protein also inhibited phagocytosis in a Csk-dependent manner, raising the possibility that this may be a general mechanism among diverse bacteria. Harnessing Csk to subvert the Fcγ receptor (FcγR)-mediated phagocytic pathway represents a new bacterial mechanism for circumventing a crucial component of the innate immune response and may potentially affect other SFK-involved cellular pathways.**

IMPORTANCE **Phagocytosis is a critical component of the immune system that enables pathogens to be contained and cleared. A number of bacterial pathogens have developed specific strategies to either physically evade phagocytosis or block the intracellular signaling required for phagocytic activity. *Haemophilus ducreyi*, a sexually transmitted pathogen, secretes a 4,153-amino-acid (aa) protein (LspA1) that effectively inhibits FcγR-mediated phagocytic activity. In this study, we show that a 294-aa domain within this bacterial protein binds to C-terminal Src kinase (Csk) and stimulates its catalytic activity, resulting in a significant attenuation of Src kinase activity and consequent inhibition of phagocytosis. The ability to inhibit phagocytosis via Csk is not unique to *H. ducreyi*, because we found that the *Helicobacter pylori* CagA protein also inhibits phagocytosis in a Csk-dependent manner. Harnessing Csk to subvert the FcγR-mediated phagocytic pathway represents a new bacterial effector mechanism for circumventing the innate immune response.**

Received 8 April 2014 **Accepted** 10 April 2014 **Published** 20 May 2014

Citation Dodd DA, Worth RG, Rosen MK, Grinstein S, van Oers NSC, Hansen EJ. 2014. The *Haemophilus ducreyi* LspA1 protein inhibits phagocytosis by using a new mechanism involving activation of C-terminal Src kinase. mBio 5(3):e01178-14. doi:10.1128/mBio.01178-14.

Editor Michele Swanson, University of Michigan

Address correspondence to Eric J. Hansen, Eric.Hansen@UTSouthwestern.edu.

This article is a direct contribution from a member of the American Academy of Microbiology.

Haemophilus ducreyi is a fastidious, Gram-negative bacterium that causes chancroid, a sexually transmitted genital ulcer disease (1). Chancroid is most prevalent in some developing countries in Africa and Asia and has been identified as a cofactor in transmission of HIV infection (for reviews, see references 2 and 3). Chancroid is exceedingly rare in the United States, although outbreaks associated with commercial sex workers have been documented (4). Humans are the only natural host for this pathogen, and chancroid remains one of the least understood sexually transmitted infections (STIs) (5, 6), despite 30 years of research efforts aimed at the identification of *H. ducreyi* virulence mechanisms (for reviews, see references 6 and 7).

Over the past two decades, a large number of putative virulence factors of this organism have been identified, including both proteins and lipo-oligosaccharide (LOS). However, subsequent testing in the human challenge model for experimental chancroid (for a review, see reference 7) revealed that only a subset of these genes were truly essential for full virulence of *H. ducreyi*. These included

lspA1 and *lspA2*, whose inactivation severely attenuated the virulence of *H. ducreyi* (8). LspA1 and LspA2 are very large proteins (456 kDa and 542 kDa, respectively) (9) secreted from *H. ducreyi* by the LspB outer membrane protein in a two-partner secretion system (10). LspA1 and LspA2 have 86% identity (9) but are regulated differently (11). *In vitro* assays demonstrated that LspA1 and LspA2 can independently inhibit Fcγ receptor (FcγR)-mediated phagocytosis in macrophage and polymorphonuclear leukocyte cell lines (12, 13).

FcγR-mediated phagocytosis is a critical component of the innate immune response that causes engulfment and clearing of antibody-coated bacteria. The phagocytic event begins when one of the Fcγ receptors recognizes an opsonized target and clusters with other Fcγ receptors (14). This clustering enables Src family protein tyrosine kinases (SFKs) to phosphorylate the Fcγ receptor immunoreceptor tyrosine-based activation motif (ITAM) domains. The phosphorylated ITAMs serve as docking sites for Src2 homology domains of the Syk protein tyrosine kinases (PTKs), enabling these to be activated. The Syk PTKs phosphorylate and activate multiple downstream pathways, leading to assembly of actin and pseudopod extension. The activation of SFKs is a critical early step for the initiation of these phagocytic signaling processes (15). Of the nine SFKs, Lyn, Hck, and Fgr are most often coupled to FcγR-mediated phagocytosis (16, 17). Myristoylated and palmitoylated SFKs partition preferentially to the inner leaflet of the plasma membrane (18). The SFKs are present primarily in two forms, an activated molecule with an extended shape that is phosphorylated on Y418 in the activation loop of the kinase domain and a more compact form that is mostly inactive and phosphorylated on Y529. The majority of SFKs within a resting mammalian cell are found in the pY529 form, and very few SFKs are in the active pY418 form (19, 20). Phosphatases such as PTPα, PTP1B, and Shp2 can activate SFKs by dephosphorylating Y529 (21, 22). The protein kinases responsible for inactivating SFKs by phosphorylating Y529 are the C-terminal Src kinase (Csk; the subject of the present study) and the C-terminal Src kinase homologous kinase (Chk) (21).

Csk, the nonreceptor C-terminal protein-tyrosine kinase that phosphorylates the Y529 negative regulatory site of SFKs, is highly conserved across the animal kingdom (23). It has three domains: an SH3 domain, an SH2 domain, and a kinase domain. These same three domain types are found in SFKs. However, unlike the SFKs, Csk is missing a phosphorylation site within the activation loop and is therefore regulated differently. Instead of being controlled by tyrosine phosphorylation, Csk adopts active and inactive conformations that are in dynamic equilibrium and are regulated by the binding of proteins to the Csk SH2 domain (23). The Csk crystal structure shows that both the SH2 and SH3 domains protrude from the molecule, enabling easy access for other proteins (24). An elegant study by Wong et al. (25) demonstrated that, when the Csk-binding protein (Cbp) binds to the SH2 domain of Csk, there is a major cantilever-type change in the molecule, resulting in an increase in enzyme activity (25). Given that activation of SFKs is critical to phagocytosis, enhancement of Csk activity would be predicted to inhibit phagocytosis. Indeed, overexpression of Csk within mammalian cells has been shown to inhibit phagocytosis (26).

Pathogenic bacteria can inhibit the FcγR-mediated phagocytic signaling pathway at multiple steps (14, 27). Several *Escherichia coli* strains, *Yersinia* spp., *Pseudomonas aeruginosa*, *Vibrio parahaemolyticus*, and *Burkholderia cenocepacia* inject effectors directly into macrophages. These factors block Rho family GTPases, function as tyrosine phosphatases, or manipulate phosphoinositides to impede phagocytosis. *H. ducreyi* expressing the LspA proteins decreases the level of active SFKs (13). However, it was unclear whether this was directly responsible for LspA-mediated inhibition of phagocytic activity, and, if so, how the LspA proteins suppressed SFK activity.

A clue to this mechanism emerged with studies showing that the LspA proteins themselves are tyrosine phosphorylated in the presence of mammalian cells (28). Incubation of wild-type *H. ducreyi* with a macrophage cell line resulted in the tyrosine phosphorylation of the LspA proteins (28). Subsequent investigation identified four tyrosine residues in LspA1 that could be phosphorylated by macrophages (28). These four LspA1 tyrosines are located in either EPIYG or EPVYA motifs. To date, only five other bacteria (*Helicobacter pylori*, *Chlamydia trachomatis*, *Bartonella henselae*, enteropathogenic *E. coli*, and *Anaplasma phagocytophilum*) have been reported to express proteins that are tyrosine phosphorylated in mammalian cells (29–31). The effector proteins (CagA, Tarp, Bep, Tir, and AnkA, respectively) from these other pathogens share an EPIYA consensus motif and are injected directly into mammalian cells by either type III or type IV secretion systems. LspA1 is presumed to enter the mammalian cell by an as-yet-undefined mechanism.

None of these EPIYA motif-containing bacterial proteins share any homology except their EPIYA motifs, suggesting that they do not come from a common ancestor (29). Because these tyrosine-phosphorylated bacterial proteins can bind different mammalian proteins (31), they can regulate varied host cell responses such as pedestal formation (Tir), cell scattering (CagA), cell invasion (Tarp), and cytokine release (CagA and Bep) (30). A BLASTP search of the EPIYA motif against the nonredundant protein database identified numerous predicted proteins of bacterial origin that possessed this motif, with only a very few eukaryotic matches. To date, the only mammalian EPIYA protein that has been characterized is pragmin, which binds Csk and minimizes its interaction with SFKs (32).

Here, we show that expression of a 37-kDa LspA1 fragment (YL2) containing two EPIYG motifs was sufficient to both inhibit FcγR-mediated phagocytosis and reduce the level of active SFKs. Both activities required phosphorylation of the tyrosines within the EPIYG motifs. Quantitative proteomics with this EPIYG-containing LspA1 fragment revealed that C-terminal Src kinase (Csk), a tyrosine kinase that negatively regulates SFKs, is the principal mammalian binding partner of this bacterial phosphoprotein. When YL2 was added to recombinant Csk in *in vitro* kinase assays, YL2 was phosphorylated and increased Csk activity over 10-fold. Phosphorylation of YL2 can be performed by SFKs and by Csk. A YL2 mutant that cannot be phosphorylated had no effect on Csk activity. Our data suggest a model in which phospho-YL2 binds and directly activates Csk. Csk activation by YL2 results in reduced levels of active SFKs and ultimately blocks phagocytosis. In addition, the CagA protein from *H. pylori* that has EPIYA motifs and binds Csk was also found to inhibit phagocytosis in a Csk-dependent manner. Taken together, our experiments reveal a new functional role for bacterial effector proteins containing EPIY(A/G) motifs in suppressing phagocytosis by activating Csk.

RESULTS

Tyrosine phosphorylation of a fragment of LspA1 is sufficient to inhibit FcγRIIA-mediated phagocytosis. To delineate the region of LspA1 responsible for the inhibition of phagocytosis, ~1-kb portions of DNA from the *lspA1* gene were cloned into mammalian expression vectors and transfected into mammalian cells competent for phagocytosis. We focused on two LspA1 segments, YL2 and YL3, each containing two tyrosines that were previously shown to be phosphorylated by macrophages (28) (Fig. 1A). A third region, L1, was utilized as a negative control because of its demonstrated lack of phosphotyrosines (28) (Fig. 1A).

Given the importance of tyrosine phosphorylation, tyrosine-to-phenylalanine substitutions were engineered in these constructs (YL2-Y2469F, YL2-Y2545F, YL3-Y3269F, YL3-Y3349F), and double mutants (DM) were also produced. All of these proteins were successfully expressed when transfected into HEK293T cells (Fig. 1B, bottom). Among L1, YL2, and YL3, only YL2 was tyrosine phosphorylated (Fig. 1B, top). Each of the single tyrosine mutants of YL2 was phosphorylated; as expected, YL2-DM was not phosphorylated (Fig. 1B, top).

These various *lspA1* constructs (with and without mutated tyrosines) were cotransfected into COS-7 cells along with a plasmid encoding the human FcγRIIA gene fused to green fluorescent protein (GFP). Expression of FcγRIIA-GFP in COS-7 cells enables these cells to become phagocytic and ingest IgG-opsonized latex beads (33). When FcγRIIA-GFP-expressing COS-7 cells were cotransfected with an empty vector or L1, phagocytosis levels were high (Fig. 1C and D). Expression of YL2 or either one of the single Y→F mutants of YL2 inhibited phagocytosis (Fig. 1C). In contrast, FcγRIIA-GFP-expressing COS-7 cells transfected with YL2-DM ingested beads at levels equivalent to COS-7 cells expressing the empty vector or the L1 construct. Figure 1E shows immunofluorescent images of phagocytosis by COS-7 cells after cotransfection with four different plasmids and the plasmid encoding FcγRIIA-GFP. These experiments (Fig. 1C) revealed that at least one of the tyrosine residues within the two EPIYG motifs in YL2 must be phosphorylated to inhibit FcγR-mediated phagocytosis. In contrast, the YL3 protein, which was not phosphorylated (Fig. 1B), did not inhibit phagocytosis (Fig. 1D).

These experiments were repeated in the naturally phagocytic macrophage cell line RAW264.7. Only enhanced GFP (EGFP)-YL2 inhibited phagocytosis (Fig. 1F). Taken together, these findings reveal a critical role for the tyrosine residues in the YL2 EPYIG motif in inhibiting phagocytic activity.

The YL2 fragment of LspA1 also inhibits activation of SFKs. Macrophages incubated with wild-type *H. ducreyi* have reduced levels of active SFKs compared to those of cells incubated with an *H. ducreyi lspA1 lspA2* mutant (13). To determine if the suppression of SFK activation was mediated by the EPYIG motif, empty vector and the L1, YL2, and YL2-DM constructs were transfected into HEK293T cells along with FcγRIIA. Consistent with our earlier experiments, only YL2 inhibited phagocytosis (Fig. 2A). The level of the active form of SFKs recognized by the pY418 antibody was reduced by YL2 expression; a similar reduction was not seen when L1 or YL2-DM was expressed (Fig. 2B). In contrast, the levels of pY529-reactive SFKs were not detectably altered regardless of which *H. ducreyi* protein was expressed.

Identification of mammalian proteins that bind YL2. To identify mammalian proteins that interact with YL2, we used a stable isotope labeling of amino acids in cell culture (SILAC) proteomic screen. HEK293T cells were metabolically labeled by growing them in medium containing stable heavy isotopes of arginine and lysine. Unlabeled cells were transfected with a plasmid encoding L1-Myc, and a plasmid encoding YL2-Myc was transfected into the labeled cells. Anti-Myc immunoprecipitates from both samples were mixed together, the combined sample was digested with trypsin, and high-resolution liquid chromatography/tandem mass spectrometry (LC/MS-MS) analysis was performed. Proteins that specifically interacted with YL2 would be more abundant in the heavy form, whereas contaminant proteins that bound both L1 and YL2 would have heavy/light ratios close to 1.

All proteins from the screen that had a normalized ratio greater than 1.7 are listed in Table 1. The mass spectrometry proteomics data have been deposited to the ProteomeXchange Consortium via the PRIDE partner repository with the dataset identifier PXD000932 (http://www.ebi.ac.uk/pride/archive/projects/PXD000932). Foremost among these was C-terminal Src kinase (Csk), with a heavy/light ratio of almost 80. Csk phosphorylates the C-terminal tyrosine on SFKs (Y529 in human c-Src) to inactivate these kinases (23). The top five proteins (Csk, Nck2, Nck1, Shp2, and Grb2) all bind tyrosine-phosphorylated proteins with EPIYA motifs from other bacteria. Because these interactions from a previous study were defined in a SILAC screen using 15-mer peptides with a centrally located tyrosine (31), the interaction involving YL2 likely involves a core sequence near the tyrosines in the EPIYG motifs. Of note, Csk was also reported to bind the *H. pylori* CagA and *B. henselae* Bep proteins (31).

To confirm the SILAC results, pulldowns were performed after expressing the top five proteins together with L1, YL2, or YL2-DM containing a C-terminal Strep tag. Both YL2 and YL2-DM coprecipitated with Csk, while L1 did not (Fig. 3A). Precipitation of Csk directly revealed a strong coprecipitation of YL2, a small amount of YL2-DM, and no L1. Similar results were seen for Nck2 and Grb2 (Fig. 3B and C). An interaction of YL2 or YL2-DM with Nck1 and Shp2 was not reproducibly detected.

Csk contains an SH3 domain, followed by an SH2 domain and a COOH-terminal kinase domain (Fig. 3D). We used coprecipitation experiments to determine which domain(s) of Csk bound YL2 (Fig. 3E). We found that the SH2 domain bound YL2 (Fig. 3E, lane 4), but the kinase domain (KD) fragment did not (Fig. 3E, lane 5). Since the SH3 domain was poorly expressed (Fig. 3E, lane 3), we were unable to determine if it interacted with YL2. It should be noted that primary regulation of Csk involves the binding of scaffolds to its SH2 domain, and proteins that bind this region can upregulate the kinase activity of Csk (23).

Csk activity is critical for the inhibition of phagocytosis by YL2. To determine whether modulation of the catalytic activity of Csk by YL2 is responsible for the inhibition of phagocytosis, a kinase-deficient (dominant-negative) Csk (Csk-DN; Fig. 3D) was constructed. Phagocytic assays were performed in COS-7 cells following transfection of FcγRIIA, YL2, or L1 and either Csk-WT, Csk-DN, or EGFP (control). Inhibition of phagocytosis by YL2 was completely dependent on the activity of Csk, as the presence of Csk-DN reversed the inhibition, with the phagocytosis index being increased to levels obtained with the L1 construct (Fig. 4A). Csk-DN expression with L1 resulted in phagocytic activity equivalent to L1 with the EGFP control construct, showing that Csk-DN does not generally increase phagocytic activity. Consis-

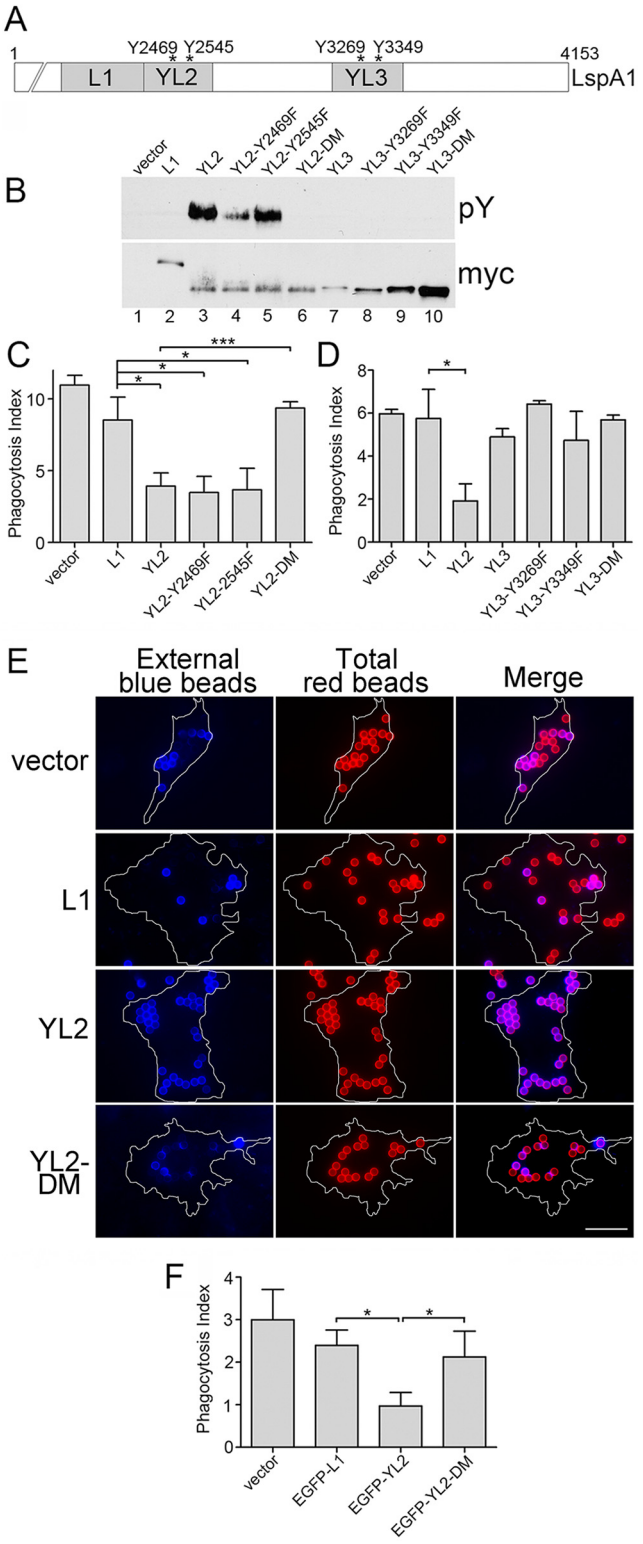

FIG 1 Inhibition of FcγR-mediated phagocytosis by fragments of LspA1. (A) Schematic showing the C-terminal half of the 4,153-aa LspA1 protein. The L1 (aa 1998 to 2348), YL2 (aa 2349 to 2643), and YL3 (aa 3149 to 3448) segments are shaded. The tyrosines that were phosphorylated when recombinant LspA1 proteins were incubated with macrophages (28) are labeled with asterisks. (B) Lysates from HEK293T cells transfected with the indicated plasmids were subjected to immunoprecipitation with anti-Myc beads. Samples were run on two gels. One gel was probed with the phosphotyrosine monoclonal antibody 4G10

(Continued)

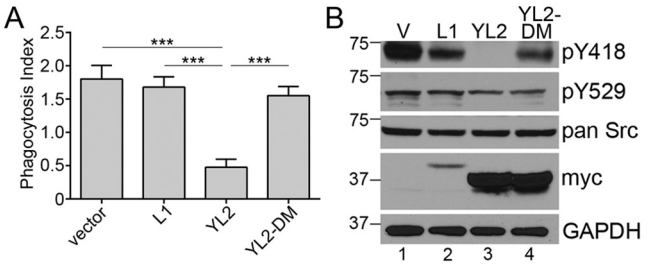

FIG 2 YL2 reduces SFK activity. (A) HEK293T cells cotransfected with either pcDNA3.1 vector (V), Myc-tagged L1, YL2, or YL2-DM constructs, and FcγRIIA-GFP were allowed to phagocytose fluorescently labeled IgG-opsonized beads. The phagocytosis index was determined for each sample. Error bars are ±SD ($n = 3$ samples) (***, $P < 0.001$). The result is representative of three independent experiments. (B) Total cell lysates (TCL) from HEK293T cells were probed in Western blot analysis with antibodies recognizing active Src (pY418), inactive Src (pY529), pan Src, Myc, or GAPDH. It should be noted that the amount of cell lysate loaded on the gel for the pY418 blot was 10-fold greater than that used for the pY529 blot.

tent with a previous report (26), overexpression of wild-type Csk inhibited FcγR-mediated phagocytosis *in vitro* (Fig. 4A).

Overexpression of either Lyn or Csk causes phosphorylation of YL2. SFKs (e.g., Lyn) are known to phosphorylate bacterial proteins with EPIYA motifs (29), including YL2 (28). However, it was unknown whether the kinase activity of Csk could phosphorylate YL2. To test this in a mammalian system, HEK293T cells were cotransfected with YL2 and either Lyn, Csk-DN, or Csk-WT. Overexpression of either Lyn or Csk-WT resulted in tyrosine phosphorylation of YL2 (Fig. 4B, top, lane 1 or 5, respectively). Csk-DN did not phosphorylate YL2. Addition of a phosphatase to the precipitates dephosphorylated YL2 (Fig. 4B, lanes 2 and 6). Interestingly, YL2 migrated more slowly when coexpressed with Lyn or Csk-WT (Fig. 4B, bottom, lane 1 or 5, respectively), and treatment with a phosphatase restored the normal electrophoretic mobility of YL2 (Fig. 4B, bottom, lanes 2 and 6).

YL2 significantly enhances Csk activity and is a substrate for Csk. To investigate whether YL2 could directly activate Csk, a tyrosine kinase assay that measures phosphorylation of a poly (Glu-Tyr) peptide was performed with recombinant Csk and recombinant YL2, YL2-DM, or L1. Increasing concentrations of YL2 increased Csk activity in a dose-dependent manner (Fig. 5). When 65 nM Csk and 50 nM YL2 were incubated together, there

Figure Legend Continued

(pY), and the other with Myc antibody (Myc). (C and D) COS-7 cells cotransfected with FcγRIIA-GFP and the indicated plasmids were allowed to ingest fluorescently labeled opsonized latex beads. The number of phagocytosed beads per cell (phagocytosis index) was quantitated for each sample. Both results are representative of three independent experiments. (E) COS-7 cells were cotransfected with FcγRIIA-GFP and the indicated plasmids. Red opsonized beads were incubated with transfected cells for 45 min. Samples were then placed on ice, and external beads were labeled blue. The plasma membrane of 1 cell for each sample is shown as a white line. Beads that bound and remained outside the cell are purple in the merge images, whereas beads that were internalized are red in the merge images. It can be seen that the COS-7 cells transfected with YL2 ingested the fewest opsonized beads. The scale bar is 20 μm. (F) RAW264.7 cells transfected with the indicated plasmids were allowed to ingest fluorescent opsonized beads, and phagocytosis ability was quantitated. The result is representative of two independent experiments. Error bars are ± standard deviation (SD) ($n = 3$ samples) (*, $P < 0.05$; **, $P < 0.01$; ***, $P < 0.001$).

TABLE 1 YL2-interacting proteins as determined by SILAC[a]

Identification partner	Symbol	UniProt	No. of identified peptides	Ratio normalized
C-Src kinase	CSK	P41240	20	78.8
Cytoplasmic protein Nck2	NCK2; GRB4; NCKbeta	O43639	8	29.2
Cytoplasmic protein Nck1	NCK1; NCK; NCKalpha	P16333	4	16.5
Tyrosine protein phosphatase nonreceptor type 11	PTPN11; SH-PTP2; SH-PTP3; SHP2	Q06124	2	11.7
Growth factor receptor-bound protein 2	GRB2	P62993	3	10.1
ATP-dependent RNA helicase A	DHX9	Q08211	1	2.4
40S ribosomal protein S23	RS23	P62266	2	2.3
100-kDa DNA pairing protein; splicing factor	SFPQ	P23246	17	1.9
54-kDa nuclear RNA- and DNA-binding protein	NONO	Q15233	15	1.9
ATP-dependent RNA helicase A 46	DHX15	O43143	1	1.8
Caprin-1	CAPR1	Q14444	8	1.7

[a] Proteins with normalized heavy/light ratios less than 1.7 are not listed.

was a 10-fold increase in Csk activity (Fig. 5A). YL2 itself had no kinase activity, and YL2-DM did not stimulate Csk activity.

YL2 was added to this kinase assay (Fig. 5A) in an unphosphorylated state. We previously showed that overexpression of Csk in mammalian cells resulted in phosphorylation of mammalian-expressed YL2 (Fig. 4B); however, this may not indicate direct phosphorylation of YL2 by Csk because many other proteins are present in the cell. To test whether purified recombinant Csk could phosphorylate purified recombinant YL2, we used conditions similar to those in the kinase assay and found that Csk can tyrosine phosphorylate YL2 in an ATP-dependent manner (Fig. 5B). These data show that unphosphorylated YL2 incubated with Csk in the presence of ATP becomes phosphorylated and thus activated.

***Helicobacter pylori* CagA inhibits phagocytosis in a Csk-dependent manner.** The *H. pylori* CagA protein contains EPIYA motifs that can be phosphorylated and bind Csk (31). In gastric adenocarcinoma cells, CagA causes a "hummingbird" phenotype wherein the cells are more elongated; this phenotype is dependent on tyrosine phosphorylation of CagA (34). CagA proteins from different *H. pylori* strains vary in the number and type of EPIYA motifs (see Table S1 in the supplemental material), and differences among CagA proteins in their induction of the hummingbird phenotype, binding of Shp2, and oncogenic potential all correlate with the number of the EPIYA motifs at these sites (35). Figure 6A shows the fragments of CagA proteins from three strains of *H. pylori* chosen for this study, with G27 having four EPIYA motifs, 26695 with three, and J99 with just two. All three of the CagA protein fragments were expressed (Fig. 6B). When the CagA fragments were independently coexpressed with the FcγRIIA receptor in COS-7 cells, all three inhibited phagocytosis, with G27 CagA being the most inhibitory (Fig. 6C). Given these findings, we examined whether the inhibition of phagocytosis by the CagA G27 protein involved Csk. Similar to results obtained with the *H. ducreyi* YL2 construct (Fig. 4A), inhibition of phagocytosis by the CagA G27 fragment was rescued by coexpression of Csk-DN (Fig. 6D).

DISCUSSION

The ability of *H. ducreyi* to inhibit phagocytosis was described over a decade ago (36, 37), yet the molecular mechanism remained incompletely understood. We demonstrate here that a 296-aa fragment (YL2) from the 4,153-aa *H. ducreyi* LspA1 protein inhibits its FcγR-mediated phagocytosis when expressed in mammalian cells. This LspA1 fragment also decreases the level of active SFKs present in the cell. At least one of the two tyrosines within the EPIYA motifs in YL2 must be phosphorylated to obtain these two effects. More importantly, we determined that Csk is the principal

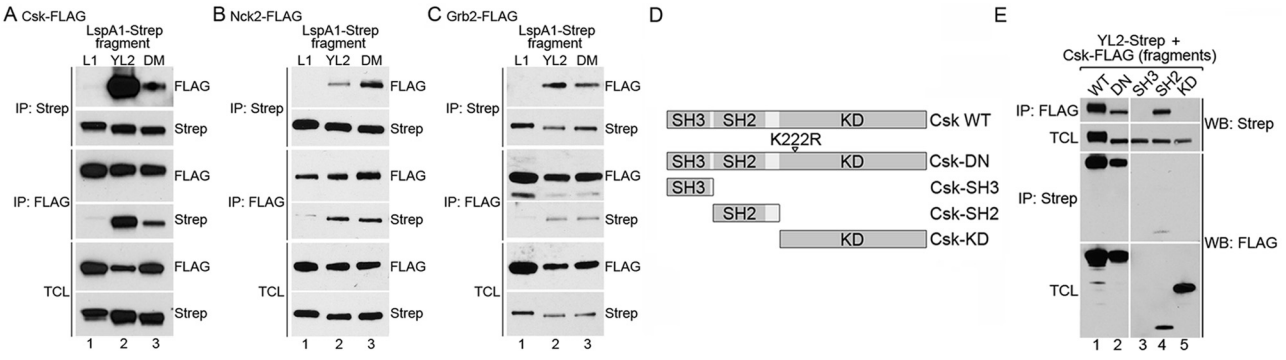

FIG 3 Pulldown-based detection of YL2-binding proteins in mammalian cells. HEK293T cells cotransfected with L1, YL2, or YL2-DM (DM) containing Strep tags and either Csk-FLAG (A), Nck2-FLAG (B), or Grb2-FLAG (C) were pulled down with either Strep-Tactin beads or FLAG antibody-coated beads. Samples of the pulldowns (IP) and total cell lysate (TCL) were run in SDS-PAGE, and then Western blotting was performed with either FLAG or Strep primary antibodies. (D) Schematic of Csk-derived constructs. (E) HEK293T cells were cotransfected with YL2-Strep and each of the Csk-derived constructs with a FLAG tag. Proteins were either pulled down with anti-FLAG or Strep-Tactin beads. Precipitates (IP) and TCL were probed in Western blot analysis with antibodies against Strep or FLAG.

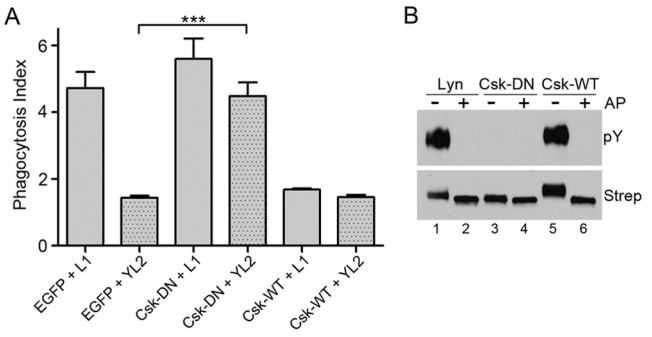

FIG 4 A dominant-negative Csk (Csk-DN) rescues phagocytosis in the presence of YL2 and is unable to phosphorylate YL2. (A) COS-7 cells cotransfected with three plasmids encoding FcγRIIA, either EGFP-L1 or EGFP-YL2, and either EGFP (control), Csk-DN, or Csk-WT had opsonized fluorescently labeled latex beads added. The phagocytosis index for each sample was quantitated. Error bars are ±SD ($n = 3$ samples) (***, $P < 0.001$). The result is representative of two independent experiments. (B) HEK293T cells were cotransfected with YL2-Strep and either Lyn, Csk-DN, or Csk-WT with a FLAG tag. YL2 was precipitated with Strep-Tactin beads. Samples were split into two portions, and one was treated with Antarctic phosphatase (AP). The paired samples were then probed in Western blot analysis with either pY or Strep antibodies.

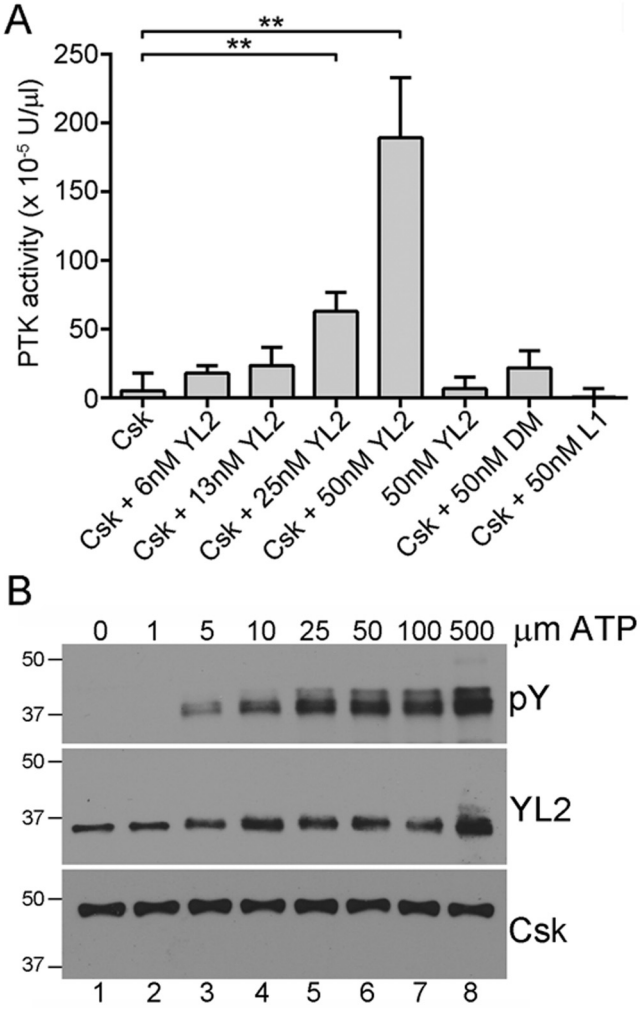

FIG 5 YL2 enhances Csk activity and is phosphorylated by Csk. (A) Recombinant Csk (65 nM) mixed with recombinant YL2 (at 6.25, 12.5, 25, or 50 nM), YL2-DM (DM) (at 50 nM), or L1 (at 50 nM) was added to wells of a universal tyrosine kinase assay containing bound poly (Glu-Tyr) peptides. Tyrosine phosphorylation of the bound peptide was detected with a horseradish peroxidase (HRP)-conjugated pY antibody, and absorbance at OD_{450} was compared to a standard curve of a PTK control provided in the kit. One unit of enzyme is the amount needed to incorporate 1 pmol of phosphate into the substrate (KVEKIGEGTYGVVYK; residues 6 to 20 of $p34^{cdc2}$) in 1 min. Error bars are ±SD ($n = 3$) (**, $P < 0.01$). The result is representative of three independent experiments. (B) Recombinant Csk (65 nM) and recombinant YL2 (50 nM) were incubated together with various concentrations of ATP. Western blots of the reactions were probed with either the phosphotyrosine monoclonal antibody 4G10 (pY), a monoclonal antibody directed against YL2, or an antibody to Csk.

mammalian protein interacting with YL2 and that YL2 dramatically enhanced Csk activity *in vitro*, thus providing a mechanism for the inhibition of SFK activation. A model for YL2-mediated inhibition of phagocytosis is depicted in Fig. 7. Both panels in Fig. 7 depict a phagocytic cell that has bound an IgG-opsonized target. In both cases, there is clustering of Fcγ receptors. When YL2 is absent (Fig. 7A), Csk is not activated. Under these conditions, the SFKs are active and phosphorylate the ITAM receptors to initiate the phagocytic signaling pathway. When YL2 is present (Fig. 7B), Csk is activated and phosphorylates Y529 in SFKs, which then do not phosphorylate the ITAM receptors, resulting in inhibition of phagocytosis.

Two different protein fragments from LspA1 (YL2 and YL3) containing EPIYA-like motifs were tested for their ability to inhibit phagocytosis in this study. We found that, when expressed in mammalian cells, only YL2 was phosphorylated (within its EPIYG motifs) and inhibited phagocytosis. It may be that YL2 is more readily phosphorylated than YL3, perhaps by binding a kinase(s) more tightly. In a previous study (28), another LspA1-derived fusion protein (GSTL) containing the same EPVYA motif as YL3 was shown to be tyrosine phosphorylated by purified Src kinase *in vitro*. However, this same GSTL fusion protein was not tyrosine phosphorylated by macrophage lysates (28). It should be noted that the experiments in the present study were performed using mammalian expression vectors to produce various segments of the bacterial LspA1 protein within eukaryotic cells. In the future, we hope to develop *H. ducreyi* constructs that produce a mutated LspA1 protein with Y→F changes in the YL2 region. While some genetic manipulation of *H. ducreyi* is possible (38, 39), the successful development of *H. ducreyi* mutants with site-directed mutations (e.g., single nucleotide changes) in the chromosome has not been reported to date.

The tyrosines within the EPIYG motifs of YL2 were clearly critical in activating Csk (Fig. 5A), although YL2-DM (which lacks these tyrosines) could still bind Csk, albeit at apparently decreased levels relative to YL2 (Fig. 3A). Despite exhibiting some binding to Csk, YL2-DM had little or no ability to activate Csk (Fig. 5A). Because binding to the Csk SH2 domain alone should activate this kinase (23), the lack of Csk activation seen with YL2-DM could be related to the apparent reduced binding. *In vitro*, recombinant YL2 alone can increase recombinant Csk activity 10-fold. Unlike Cbp, which must be added to kinase assays in a phosphorylated form to activate Csk, YL2 was added to the assays in the present study as an unphosphorylated protein (and was presumably phosphorylated *in situ* as shown in a separate *in vitro* assay [Fig. 5B]). Csk has been reported to have extremely high specificity for SFKs,

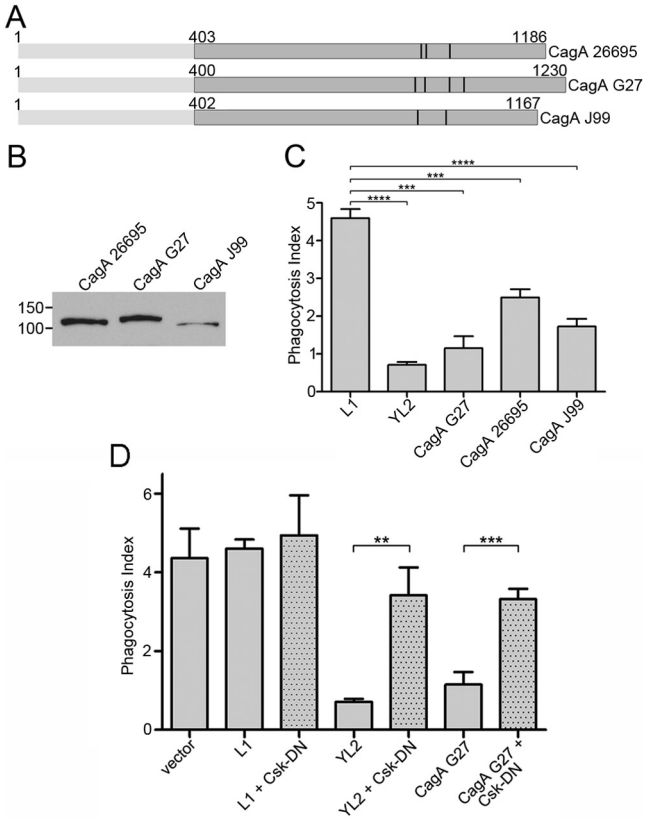

FIG 6 CagA from *H. pylori* inhibits phagocytosis in a Csk-dependent manner. (A) Schematic of the CagA proteins from three strains of *H. pylori*. The darker portions from approximately aa 400 to the C-terminal end were the sections of the corresponding *cagA* genes that were cloned into the mammalian expression vector. Dark vertical lines indicate where EPIYA motifs are located. (B) Western blot analysis showing expression of the CagA fusion proteins as detected by probing with GFP antibody. (C) Phagocytosis indices obtained for COS-7 cells cotransfected with FcγRIIA and L1, YL2, or the three different CagA constructs. The result is representative of three independent experiments. (D) COS-7 cells were cotransfected with FcγRIIA-GFP and either vector, L1, YL2, or the G27 CagA construct. For three samples, Csk-DN was also cotransfected. Both YL2 and G27 CagA inhibited phagocytosis, and this inhibition was alleviated by the expression of Csk-DN. Error bars are ±SD ($n = 3$ samples) (**, $P < 0.01$; ***, $P < 0.001$; ****, $P < 0.0001$). These results are all representative of three independent experiments.

even when overexpressed (40), so it was surprising that Csk phosphorylated YL2. Our data suggest that YL2 can be activated (phosphorylated) by the kinase that it activates (Csk), resulting in positive feedback and strong Csk activation.

SFKs are key players in the signal transduction pathway for FcγR-mediated phagocytosis, with Csk functioning as a negative regulator of SFKs. Csk phosphorylates the inhibitory Y529 residue of SFKS. SFKs essentially toggle between an inactive state where Y529 is phosphorylated and Y418 is not phosphorylated and an active state where Y529 is not phosphorylated and Y418 is phosphorylated. However, in resting cells, inactive SFKs with phosphorylated Y529 are the predominant form, and there are many fewer molecules in the active confirmation with Y418 phosphorylated (19, 20). Consistent with this idea, we needed to load at least 10-fold more cell lysate to detect pY418 SFK molecules than we did to detect pY529 SFKs in Western blots (Fig. 2B). We predicted that there would be increased levels of pY529 SFKs and decreased levels of pY418 SFKs in cells expressing YL2, which activates Csk, which in turn phosphorylates Y529, resulting in a decrease in pY418-active SFKs. Examination of mammalian cells overexpressing YL2 (which now have activated Csk) showed that pY418-active SFKs were obviously decreased, whereas the pY529 levels apparently remained steady (Fig. 2B). The latter result was contrary to our expectation but likely reflects the fact that the abundance of pY529 levels makes detection of a small increase in pY529 SFKs difficult. In contrast, the much smaller amounts of active pY418 SFKs in these cells facilitate detection of even a small decrease in pY418 SFKs.

Incubation of wild-type *H. ducreyi* bacteria with macrophages yielded LspA proteins that were tyrosine phosphorylated (28), a result which indicates that at least the YL2 region of the LspA1 protein must gain access to the cell cytoplasm. This previous study also showed that phosphorylation of the LspA proteins by mammalian cells was inhibited by the protein kinase inhibitor PP2, which coincidentally also inhibits Csk activity, albeit less effectively (41). Therefore, while both SFKs (28) and Csk (Fig. 5) can phosphorylate YL2 *in vitro*, we cannot determine at this time whether either or both of these kinases are responsible for phosphorylation of LspA in mammalian cells incubated with wild-type *H. ducreyi*. To date, we have not succeeded in detecting LspA proteins within macrophages after incubation of wild-type *H. ducreyi* with these mammalian cells. This is likely because only extremely minute quantities of the LspA proteins are produced by wild-type *H. ducreyi* in culture.

While numerous papers have detailed studies of *H. pylori* CagA EPIYA motifs, including the binding of Csk by CagA, we definitively show here that CagA possesses a heretofore unknown ability to inhibit FcγR-mediated phagocytosis. This inhibition depends on a functional Csk and likely works similarly to YL2-mediated inhibition. CagA-mediated inhibition of phagocytosis represents an unexplored aspect of the virulence potential of *H. pylori* and adds yet another functional dimension to this already multifaceted protein. Because the Bep proteins of *Bartonella henselae* also contain EPIYA motifs and are known to bind Csk (31), it is possible that they also possess the ability to inhibit phagocytosis.

One related and important question that remains unanswered is how the LspA1 protein gains entrance into the mammalian cell. All of the other bacterial EPIYA effector proteins described to date use either type III (e.g., enteropathogenic *E. coli*) or type IV (e.g., *H. pylori*) secretion systems to gain access to the eukaryotic cell. *H. ducreyi* does not have type III or type IV secretion systems. In addition, it has been established that wild-type *H. ducreyi* cell-free culture supernatant containing LspA1 and LspA2 inhibits phagocytosis (12). Immunodepletion of the LspA proteins from the culture supernatant removed the inhibitory activity (13), confirming that direct injection of the LspA1 protein from *H. ducreyi* into the phagocyte is not required.

Instead of using an injection method, some bacterial toxins, including botulinum toxin, cholera toxin, anthrax toxin, and the clostridial glucosylating toxins, enter eukaryotic cells by binding a receptor(s) on the cell surface and are then endocytosed into the cells (42). In contrast, the very large multifunctional-autoprocessing RTX (MARTX) toxins that vary in size from 350 kDa to 600 kDa can translocate into cells even in the presence of endocytosis inhibitors. It is hypothesized that the repeats in MARTX can form a pore-type structure that allows transfer of the effector domains into the cytosol (43). These domains are auto-

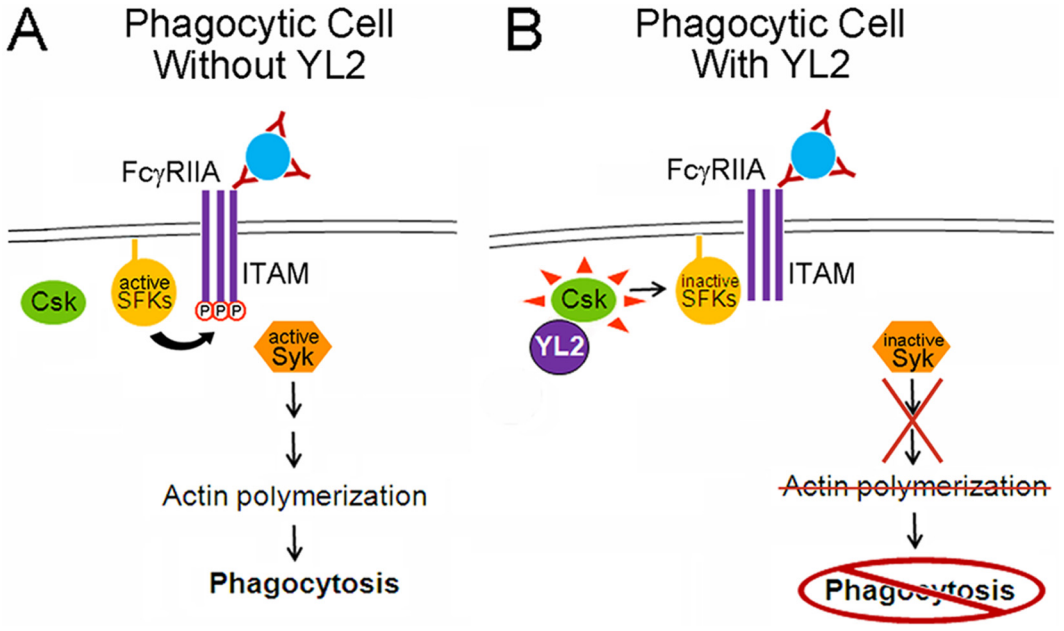

FIG 7 A model for YL2 inhibition of FcγRIIA-mediated phagocytosis. (A) In a typical phagocytic cell, IgG-opsonized targets bind to FcγRIIA receptors, resulting in clustering of these receptors and activation of SFKs. These active SFKs phosphorylate the ITAM domains of the receptors. When the ITAMs are phosphorylated, Syk kinases will be activated and a multistep signal transduction pathway ensues, ultimately resulting in actin polymerization and phagocytosis. (B) When the YL2 portion of the *H. ducreyi* LspA1 protein is present in the phagocytic cell, it binds Csk and thereby stimulates the kinase activity of Csk. The increased Csk kinase activity results in the inactivation of SFKs. Without active SFKs, the ITAMs are not effectively phosphorylated, Syk kinase is not activated, and phagocytosis cannot proceed.

processed once inside the cell to release the effectors which are involved in actin rearrangement and Rho GTPase inactivation. Many of the aforementioned toxins can be cleaved by extracellular proteases such as furin or can be cleaved after entry into the endosome by pH-sensitive proteases. Given the extremely large size of the LspA1 protein, it seems likely that it would be cleaved at some point either before, during, or after entry to allow effector domain(s) unhindered access to cytosolic or membrane targets.

The current study demonstrates, for the first time, that a relatively small region of the LspA1 protein containing EPIYA-like motifs is both necessary and sufficient to inhibit phagocytosis and that it does so by binding and activating Csk, a negative regulator of SFK activity. Phosphorylation of tyrosines within the EPIYG motifs in this fragment is critical for the inhibition of both SFK activity and phagocytosis. Exploiting Csk to restrain the FcγR-mediated phagocytic pathway represents a new bacterial mechanism for impeding a critical component of innate immunity. In addition, because SFKs regulate many signal transduction pathways within different kinds of cells, it may be that other important cellular functions are disrupted by LspA1 activating Csk, including antigen receptor signaling. Finally, given the extremely large size of the LspA proteins (9), it is an intriguing possibility that there may be additional, as-yet-undiscovered effector functions encoded within these molecules.

MATERIALS AND METHODS

Mammalian cells. RAW264.7, COS-7, and HEK293T cells (American Type Culture Collection) were grown in Dulbecco's modified Eagle's medium (DMEM) (Invitrogen) with 10% fetal bovine serum (FBS; Gemini) except as specified.

Mammalian expression constructs. Human FcγRIIA cDNA was excised using HindIII and SacII from a previously described pcDNA3.1-derived plasmid (44). The purified product was ligated into pEGFP-N1 (Invitrogen) (45). The FcγRIIA-GFP construct was verified by restriction digestion and sequencing. Protein expression was verified by flow cytometry and fluorescence microscopy. All experiments involving FcγRIIA in this study used this construct. All other constructs made for this study are described in Table S2 in the supplemental material. Oligonucleotide primers are listed in Table S3 in the supplemental material.

Western blot methods. Cells were plated and transfection was performed using Lipofectamine 2000 (Invitrogen) according to the manufacturer's instructions. Twenty-four h after transfection, cells were placed on ice, scraped into medium, and centrifuged at 1,000 × *g* for 5 min at 4°C. The pellets were washed twice with ice-cold phosphate-buffered saline (PBS) and then suspended in RIPA buffer containing protease inhibitors (Complete tablet; Roche), 1 mM phenylmethylsulfonyl fluoride (PMSF), and 1 mM sodium orthovanadate and left on ice for 10 min. After centrifugation for 10 min at 10,000 × *g*, the supernatant was placed in a new tube, loading buffer was added, and samples were boiled and then subjected to SDS-PAGE in a 10% polyacrylamide separating gel. Western blotting was done using polyvinylidene difluoride (PVDF) (Millipore). Membranes were dried and blocked with 5% bovine serum albumin (BSA) in Tris-buffered saline–Tween 20 (TBS-T) with 5% donkey serum (for the blots probed with the pY-reactive monoclonal antibody 4G10, pY418, and pY529 antibodies) or starting block (PBS) (Thermo) with 5% donkey serum (for all other antibodies used). The YL2-reactive monoclonal antibody 3H9 was described previously (28). Primary antibodies against the Myc tag (Millipore), pY (4G10; Millipore), pY418 (Invitrogen), pY529 (Invitrogen), pan Src (Invitrogen), the Strep tag (IBA), the FLAG tag (Sigma), GFP (Abcam), GAPDH (Abcam), and YL2 (3H9) were diluted in blocking buffer and typically incubated on the blots overnight at 4°C. Membranes were washed with PBS containing 0.05% Tween 20. Blots were then incubated in secondary antibodies, either peroxidase-conjugated donkey anti-mouse or anti-rabbit (Jackson ImmunoResearch) diluted in blocking buffer, washed again, and then SuperSignal West Pico chemiluminescent substrate was added (Thermo).

Src and tyrosine phosphorylation assays. HEK293T cells, split 2 days prior to each experiment onto 60-mm-diameter plates, were transfected the day before the experiment with plasmids using Lipofectamine 2000 (Invitrogen). The next day, cells were placed on ice, scraped into 1 ml ice-cold PBS, and placed in a microcentrifuge tube. After being washed once more with PBS, the cell pellet was suspended in lysis buffer (25 mM Tris [pH 7.6], 150 mM NaCl, 1% Triton X-100, 2 mM EDTA, protease inhibitors [Complete tablets; Roche], 1 mM PMSF, and 1 mM sodium orthovanadate), using 50 μl for the Src phosphorylation samples and 500 μl for tyrosine phosphorylation samples, and incubated on ice for 10 min. Samples were centrifuged for 10 min at 10,000 $\times$ *g* at 4°C. Supernatants were transferred to a new tube. Src phosphorylation samples had loading buffer added. For the tyrosine phosphorylation study, Myc-tagged proteins were immunoprecipitated with 50 μl of anti-Myc agarose conjugate (Millipore) and samples were rotated for 4 h at 4°C. After being washed 3 times with lysis buffer and aspirating liquid with a 27-gauge needle, the agarose beads were resuspended in 40 μl loading buffer. All samples were boiled for 5 min and run in two sets in SDS-PAGE. Proteins were blotted onto PVDF membranes. For the tyrosine phosphorylation study, one blot was probed with antibody 4G10 (Millipore) to detect pY residues, while the other blot was probed with a Myc antibody (Millipore). For the Src phosphorylation study, one blot was probed with anti-pY418 Src (Invitrogen), and the other was probed with anti-pY529 Src (Invitrogen). Sample equivalence for the Src phosphorylation study was confirmed by probing with anti-GAPDH (Abcam).

Phagocytosis assays. COS-7, HEK293T, and RAW264.7 cells were plated at 9×10^4 cells/ml, 2×10^5 cells/ml, and 1.5×10^5 cells/ml, respectively, in 4-well chamber slides (Fisher). Chamber slides for HEK293T cells were coated with poly-L-lysine (Sigma) prior to plating. COS-7, HEK293T, or RAW264.7 cells were transfected for 24 h with XtremeGeneHP (Roche) according to the manufacturer's instructions. The day before the experiment, latex beads (3.87-μm diameter) (Bangs Laboratories) were opsonized with human IgG by washing a 40% slurry of beads twice with PBS and then mixing overnight with 300 μg of human IgG (Jackson ImmunoResearch). The day of the experiment, opsonized beads were washed 3 times with PBS and suspended in 500 μl PBS. Anti-human Cy3 antibody (7.5 μg) (Jackson ImmunoResearch) was added to label all opsonized beads red, and the suspension was rotated end-over-end at room temperature for 1 h. After being washed 4 times with PBS, the beads were suspended in either 1 ml (for COS-7 and HEK293T cells) or 0.5 ml (RAW264.7 cells) of DMEM with 10% FBS. Cy-3-stained opsonized beads (5 μl for COS-7 and HEK293T cells or 10 μl for RAW264.7 cells) were added to the chamber slides, and the slides were centrifuged at 300 $\times$ *g* for 1 min before being placed at 37°C with 90% air-10% CO_2 for 5 min (RAW264.7 cells) or 45 min (COS-7 and HEK293T cells). The RAW264.7 cells were washed 2 times with medium and placed back into the incubator for 10 min. All slides were then placed on ice and washed with ice-cold medium. A 7.5-μg portion of anti-human Dylight 405 was added, and the slides were held for 10 min on ice in order to label extracellular beads blue. Cells were then washed 5 times with ice-cold PBS and fixed with 3.7% paraformaldehyde for 20 min. Cells were next washed twice with PBS and incubated for 10 min with 100-mM glycine. All samples were washed twice with PBS, and PBS was left in the chamber slides. Cells and beads were counted with an inverted fluorescence microscope. At least 100 green cells per well were counted, as were the number of blue extracellular beads and the number of total beads (red). The phagocytosis index was determined by subtracting the number of extracellular beads from the total beads, divided by the number of cells. In all experiments, three wells were used for each sample.

FLAG, Strep, and Myc pulldown experiments. Cells were plated and transfected, and lysates were prepared as in the Western blot experiments, except each sample had 1 ml of lysis buffer added per sample. A 30-μl portion of each sample was kept for a lysate-only control. The FLAG and Strep samples were precleared with mouse IgG anti-Myc antibody (Roche) for 2 h at 4°C with rotation. Protein A/G Plus agarose (30 μl) was added for 2 h at 4°C with rotation. Samples were then centrifuged, and the cleared supernatants were transferred to a new cold tube. Lysates were split into two tubes with 450 μl in each, either EZview Red anti-FLAG M2 affinity gel (Sigma) or Strep-Tactin Superflow Plus beads (IBA or Qiagen) were added, and samples were rotated overnight at 4°C. Samples were then washed in ice-cold lysis buffer, and the Strep samples were washed with Strep tag washing buffer (IBA). All samples were aspirated with a 27-gauge needle to remove excess liquid, and either loading buffer or Strep tag elution buffer (IBA) followed by loading buffer was added. The Myc-based immunoprecipitations were performed similarly except that the cell pellets were brought up in 500 μl lysate and there was no preclearing necessary. For these samples, 50 μl of Myc tag antibody (clone 4A6 agarose conjugate; Millipore) was used.

SILAC pulldown. HEK293T cells were grown in lysine- and arginine-free DMEM (Thermo) with 10% dialyzed fetal bovine serum (Thermo) supplemented with either "heavy" $^{13}C_6$ L-lysine (73 mg/liter), $^{13}C_5{}^{15}N_4$ L-arginine (42 mg/liter), and L-proline (200 mg/liter) (Thermo) or "light" corresponding nonlabeled amino acids. Each heavy and light set was grown for 6 cell doublings. Heavy cells were transfected with a plasmid encoding YL2 with a C-terminal Myc tag, and light cells were transfected with a plasmid encoding L1 with a C-terminal Myc tag, using Lipofectamine 2000 (Invitrogen) according to the manufacturer's instructions. After 24 h, cells were washed with PBS and lysed in 25 mM Tris (pH 7.6), 150 mM NaCl, 1% Triton X-100, 2 mM EDTA, protease inhibitors (Complete tablet; Roche), 1 mM PMSF, and 1 mM sodium orthovanadate. Cleared lysates were incubated with anti-Myc tag agarose conjugate (Millipore) and rotated overnight at 4°C. Samples were washed with lysis buffer and suspended in loading buffer, boiled for 5 min, and loaded on a 4% to 20% Criterion gel (Bio-Rad). Proteins within the gel were labeled with Coomassie blue stain, excised, and sliced into 1-mm pieces.

SILAC proteolytic digestion. Coomassie blue stain was removed from gel pieces by incubating for 30 min at 37°C in 50 mM triethylammonium bicarbonate (TEAB)-acetonitrile (1:1). Gel pieces were then dehydrated with acetonitrile at room temperature, followed by reduction/alkylation using dithiothreitol (DTT) and iodoacetamide. Gel pieces were dehydrated with acetonitrile and rehydrated in a solution of trypsin (10 μg/ml) in 0.05% AcOH. The digestion was carried out at 37°C overnight. Peptides were extracted at 37°C for 30 min using the extraction buffer (50% acetonitrile and 3.3% trifluoroacetic acid [TFA]). All the steps outlined above were carried out on a thermomixer shaker (Eppendorf) unless stated otherwise. Extracts were then dried using a speed vacuum concentrator and resuspended in 0.1% TFA. Salts were removed using an Oasis HLB μElution plate (Waters) before LC/MS-MS analysis.

SILAC LC/MS-MS and data analysis. MS-MS data were acquired using an Orbitrap Elite mass spectrometer (Thermo, Bremen) coupled to an Ultimate 3000-RSLCnano high-performance liquid chromatography (HPLC) system (Dionex, Santa Clara CA). Peptides were loaded onto a 180-μm (internal diameter) by 10-cm column packed in house with a reverse-phase material, C_{18} 3-μm resin (Phenomenex, Torrance, CA). Separation of peptides was carried out at 400 nl/min by a 40-min linear gradient of 1% to 41% acetonitrile in 0.1% formic acid. Mass spectra were acquired using a data-dependent acquisition method with full MS scans acquired at 240-K resolution in the Orbitrap followed by 13 data-dependent MS-MS scans acquired in the linear ion trap in the rapid mode. LC/MS-MS data were analyzed using MaxQuant (version 1.3.0.5) (46) with default parameters except that Ile-Leu equivalence was disabled. The UniprotKB human whole proteome release 2012_04 was used as the reference sequence database (47).

Phosphatase experiments. Transfected HEK293T lysates were precipitated using Strep-Tactin as described above. Samples were split into two tubes. One tube had 50 μM $MgCl_2$ and 1 μl Antarctic phosphatase (NEB) added and was incubated at 37°C for 20 min. The other tube had an equivalent amount of water added and was placed on ice. All samples then

had loading dye added. Western blot analysis was performed as described above.

Kinase assay. Recombinant YL2, YL2-DM, and L1 (previously designated HL8, Y133/209F, and HL7, respectively) were produced as described (13, 28). Recombinant baculovirus-produced Csk was purchased (Abcam). The universal tyrosine kinase assay was performed as described by the manufacturer (TaKaRa) with the following changes. Because mammalian cells were not used, the extraction buffer provided by the kit was not utilized. In addition, the recombinant proteins were incubated in 50 mM Tris-HCl (pH 7.4), 1 mM $MgCl_2$, 1 mM $MnCl_2$, and 250 mM NaCl with no addition of 2-mercaptoethanol, instead of the kinase reaction buffer provided with the kit.

***In vitro* phosphorylation assay.** Recombinant Csk (65 nM) and recombinant YL2 (50 nM) were incubated in the kinase reaction buffer described immediately above along with various concentrations of ATP (0, 1, 5, 10, 25, 50, 100, or 500 nM). Samples were incubated at 30°C for 10 min. Western blot analysis of the reaction mixtures was performed as described above.

SUPPLEMENTAL MATERIAL

Supplemental material for this article may be found at http://mbio.asm.org/lookup/suppl/doi:10.1128/mBio.01178-14/-/DCSupplemental.

Table S1, DOCX file, 0.1 MB.

Table S2, DOCX file, 0.1 MB.

Table S3, DOCX file, 0.1 MB.

ACKNOWLEDGMENTS

This work was supported by the National Institute of Allergy and Infectious Diseases grant AI32011 to E.J.H. and by grants MOP7075 and MOP93634 of the Canadian Institutes for Health Research to S.G.

The authors declare no conflict of interest.

We thank David Hendrixson for providing genomic DNA from *H. pylori* strains G27 and J99. Plasmid p4ToGA was a gift from Neal Alto. Hamid Mirzaei, David Trudgian, and Xiaofeng Guo at the UT Southwestern Proteomics Core were instrumental in performing the digestion, LC/MS-MS analysis, and data acquisition for the SILAC experiment. We thank Wei Liu for constructing the Myc-tagged L1 and YL2 expression constructs and for purifying recombinant YL2. Special thanks to Lora Hooper for carefully reading the manuscript.

REFERENCES

1. **Al-Tawfiq JA, Spinola SM.** 2002. *Haemophilus ducreyi*: clinical disease and pathogenesis. Curr. Opin. Infect. Dis. **15:**43–47. http://dx.doi.org/10.1097/00001432-200202000-00008.
2. **Bong CT, Bauer ME, Spinola SM.** 2002. *Haemophilus ducreyi*: clinical features, epidemiology, and prospects for disease control. Microbes Infect. **4:**1141–1148. http://dx.doi.org/10.1016/S1286-4579(02)01639-8.
3. **Ronald AR, Albritton W.** 1990. Chancroid and *Haemophilus ducreyi*, p 263–271. *In* Holmes KK, Mardh PA, Sparling PF, Wiesner PJ (ed), Sexually transmitted diseases, 2nd ed. McGraw-Hill, New York, NY.
4. **Haydock AK, Martin DH, Morse SA, Cammarata C, Mertz KJ, Totten PA.** 1999. Molecular characterization of *Haemophilus ducreyi* strains from Jackson, Mississippi and New Orleans, Louisiana. J. Infect. Dis. **179:**1423–1432. http://dx.doi.org/10.1086/314771.
5. **Spinola SM, Bauer ME, Munson RS, Jr..** 2002. Immunopathogenesis of *Haemophilus ducreyi* infection (chancroid). Infect. Immun. **70:**1667–1676. http://dx.doi.org/10.1128/IAI.70.4.1667-1676.2002.
6. **Janowicz DM, Li W, Bauer ME.** 2010. Host-pathogen interplay of *Haemophilus ducreyi*. Curr. Opin. Infect. Dis. **23:**64–69. http://dx.doi.org/10.1097/QCO.0b013e328334c0cb.
7. **Janowicz DM, Ofner S, Katz BP, Spinola SM.** 2009. Experimental infection of human volunteers with *Haemophilus ducreyi*: fifteen years of clinical data and experience. J. Infect. Dis. **199:**1671–1679. http://dx.doi.org/10.1086/598966.
8. **Janowicz DM, Fortney KR, Katz BP, Latimer JL, Deng K, Hansen EJ, Spinola SM.** 2004. Expression of the LspA1 and LspA2 proteins by *Haemophilus ducreyi* is required for virulence in human volunteers. Infect. Immun. **72:**4528–4533. http://dx.doi.org/10.1128/IAI.72.8.4528-4533.2004.
9. **Ward CK, Lumbley SR, Latimer JL, Cope LD, Hansen EJ.** 1998. *Haemophilus ducreyi* secretes a filamentous hemagglutinin-like protein. J. Bacteriol. **180:**6013–6022.
10. **Ward CK, Mock JR, Hansen EJ.** 2004. The LspB protein is involved in the secretion of the LspA1 and LspA2 proteins by *Haemophilus ducreyi*. Infect. Immun. **72:**1874–1884. http://dx.doi.org/10.1128/IAI.72.4.1874-1884.2004.
11. **Labandeira-Rey M, Mock JR, Hansen EJ.** 2009. Regulation of expression of the *Haemophilus ducreyi* LspB and LspA2 proteins by CpxR. Infect. Immun. **77:**3402–3411. http://dx.doi.org/10.1128/IAI.00292-09.
12. **Vakevainen M, Greenberg S, Hansen EJ.** 2003. Inhibition of phagocytosis by *Haemophilus ducreyi* requires expression of the LspA1 and LspA2 proteins. Infect. Immun. **71:**5994–6003. http://dx.doi.org/10.1128/IAI.71.10.5994-6003.2003.
13. **Mock JR, Vakevainen M, Deng K, Latimer JL, Young JA, van Oers NS, Greenberg S, Hansen EJ.** 2005. *Haemophilus ducreyi* targets Src family protein tyrosine kinases to inhibit phagocytic signaling. Infect. Immun. **73:**7808–7816. http://dx.doi.org/10.1128/IAI.73.12.7808-7816.2005.
14. **Flannagan RS, Jaumouillé V, Grinstein S.** 2012. The cell biology of phagocytosis. Annu. Rev. Pathol. **7:**61–98. http://dx.doi.org/10.1146/annurev-pathol-011811-132445.
15. **Berton G, Mócsai A, Lowell CA.** 2005. Src and Syk kinases: key regulators of phagocytic cell activation. Trends Immunol. **26:**208–214. http://dx.doi.org/10.1016/j.it.2005.02.002.
16. **Fitzer-Attas CJ, Lowry M, Crowley MT, Finn AJ, Meng F, DeFranco AL, Lowell CA.** 2000. Fcgamma receptor-mediated phagocytosis in macrophages lacking the Src family tyrosine kinases Hck, Fgr, and Lyn. J. Exp. Med. **191:**669–682. http://dx.doi.org/10.1084/jem.191.4.669.
17. **Lowell CA.** 2004. Src-family kinases: rheostats of immune cell signaling. Mol. Immunol. **41:**631–643. http://dx.doi.org/10.1016/j.molimm.2004.04.010.
18. **Resh MD.** 1994. Myristylation and palmitylation of Src family members: the fats of the matter. Cell **76:**411–413. http://dx.doi.org/10.1016/0092-8674(94)90104-X.
19. **Roskoski R, Jr..** 2004. Src protein-tyrosine kinase structure and regulation. Biochem. Biophys. Res. Commun. **324:**1155–1164. http://dx.doi.org/10.1016/j.bbrc.2004.09.171.
20. **Bjorge JD, Jakymiw A, Fujita DJ.** 2000. Selected glimpses into the activation and function of Src kinase. Oncogene **19:**5620–5635. http://dx.doi.org/10.1038/sj.onc.1203923.
21. **Frame MC.** 2002. Src in cancer: deregulation and consequences for cell behaviour. Biochim. Biophys. Acta **1602:**114–130. http://dx.doi.org/10.1016/S0304-419X(02)00040-9.
22. **Roskoski R, Jr..** 2005. Src kinase regulation by phosphorylation and dephosphorylation. Biochem. Biophys. Res. Commun. **331:**1–14. http://dx.doi.org/10.1016/j.bbrc.2005.03.012.
23. **Okada M.** 2012. Regulation of the SRC family kinases by Csk. Int. J. Biol. Sci. **8:**1385–1397. http://dx.doi.org/10.7150/ijbs.5141.
24. **Ogawa A, Takayama Y, Sakai H, Chong KT, Takeuchi S, Nakagawa A, Nada S, Okada M, Tsukihara T.** 2002. Structure of the carboxyl-terminal Src kinase, Csk. J. Biol. Chem. **277:**14351–14354. http://dx.doi.org/10.1074/jbc.C200086200.
25. **Wong L, Lieser SA, Miyashita O, Miller M, Tasken K, Onuchic JN, Adams JA, Woods VL, Jr, Jennings PA.** 2005. Coupled motions in the SH2 and kinase domains of Csk control Src phosphorylation. J. Mol. Biol. **351:**131–143. http://dx.doi.org/10.1016/j.jmb.2005.05.042.
26. **Suzuki T, Kono H, Hirose N, Okada M, Yamamoto T, Yamamoto K, Honda Z.** 2000. Differential involvement of Src family kinases in Fc gamma receptor-mediated phagocytosis. J. Immunol. **165:**473–482. http://dx.doi.org/10.4049/jimmunol.165.1.473.
27. **Sarantis H, Grinstein S.** 2012. Subversion of phagocytosis for pathogen survival. Cell Host Microbe **12:**419–431. http://dx.doi.org/10.1016/j.chom.2012.09.001.
28. **Deng K, Mock JR, Greenberg S, van Oers NS, Hansen EJ.** 2008. *Haemophilus ducreyi* LspA proteins are tyrosine phosphorylated by macrophage-encoded protein tyrosine kinases. Infect. Immun. **76:**4692–4702. http://dx.doi.org/10.1128/IAI.00513-08.
29. **Hayashi T, Morohashi H, Hatakeyama M.** 2013. Bacterial EPIYA effectors—where do they come from? What are they? Where are they going? Cell. Microbiol. **15:**377–385. http://dx.doi.org/10.1111/cmi.12040.
30. **Backert S, Selbach M.** 2005. Tyrosine-phosphorylated bacterial effector

proteins: the enemies within. Trends Microbiol. **13:**476–484. http://dx.doi.org/10.1016/j.tim.2005.08.002.
31. **Selbach M, Paul FE, Brandt S, Guye P, Daumke O, Backert S, Dehio C, Mann M.** 2009. Host cell interactome of tyrosine-phosphorylated bacterial proteins. Cell. Host Microbe **5:**397–403. http://dx.doi.org/10.1016/j.chom.2009.03.004.
32. **Safari F, Murata-Kamiya N, Saito Y, Hatakeyama M.** 2011. Mammalian Pragmin regulates Src family kinases via the Glu-Pro-Ile-Tyr-Ala (EPIYA) motif that is exploited by bacterial effectors. Proc. Natl. Acad. Sci. U. S. A. **108:**14938–14943. http://dx.doi.org/10.1073/pnas.1107740108.
33. **Tollis S, Dart AE, Tzircotis G, Endres RG.** 2010. The zipper mechanism in phagocytosis: energetic requirements and variability in phagocytic cup shape. BMC Syst. Biol. **4:**149. http://dx.doi.org/10.1186/1752-0509-4-149.
34. **Backert S, Moese S, Selbach M, Brinkmann V, Meyer TF.** 2001. Phosphorylation of tyrosine 972 of the *Helicobacter pylori* CagA protein is essential for induction of a scattering phenotype in gastric epithelial cells. Mol. Microbiol. **42:**631–644.
35. **Hatakeyama M, Higashi H.** 2005. *Helicobacter pylori* CagA: a new paradigm for bacterial carcinogenesis. Cancer Sci. **96:**835–843. http://dx.doi.org/10.1111/j.1349-7006.2005.00130.x.
36. **Wood GE, Dutro SM, Totten PA.** 2001. *Haemophilus ducreyi* inhibits phagocytosis by U-937 cells, a human macrophage-like cell line. Infect. Immun. **69:**4726–4733. http://dx.doi.org/10.1128/IAI.69.8.4726-4733.2001.
37. **Ahmed HJ, Johansson C, Svensson LA, Ahlman K, Verdrengh M, Lagergård T.** 2002. *In vitro* and *in vivo* interactions of *Haemophilus ducreyi* with host phagocytes. Infect. Immun. **70:**899–908. http://dx.doi.org/10.1128/IAI.70.2.899-908.2002.
38. **Hansen EJ, Latimer JL, Thomas SE, Helminen M, Albritton WL, Radolf JD.** 1992. Use of electroporation to construct isogenic mutants of *Haemophilus ducreyi*. J. Bacteriol. **174:**5442–5449.
39. **Spinola SM, Fortney KR, Baker B, Janowicz DM, Zwickl B, Katz BP, Blick RJ, Munson RS, Jr..** 2010. Activation of the CpxRA system by deletion of *cpxA* impairs the ability of *Haemophilus ducreyi* to infect humans. Infect. Immun. **78:**3898–3904. http://dx.doi.org/10.1128/IAI.00432-10.
40. **Levinson NM, Seeliger MA, Cole PA, Kuriyan J.** 2008. Structural basis for the recognition of c-Src by its inactivator Csk. Cell **134:**124–134. http://dx.doi.org/10.1016/j.cell.2008.05.051.
41. **Bain J, McLauchlan H, Elliott M, Cohen P.** 2003. The specificities of protein kinase inhibitors: an update. Biochem. J. **371:**199–204. http://dx.doi.org/10.1042/BJ20021535.
42. **Egerer M, Satchell KJ.** 2010. Inositol hexakisphosphate-induced autoprocessing of large bacterial protein toxins. PLoS Pathog. **6:**e1000942. http://dx.doi.org/10.1371/journal.ppat.1000942.
43. **Satchell KJ.** 2007. MARTX, multifunctional autoprocessing repeats-in-toxin toxins. Infect. Immun. **75:**5079–5084. http://dx.doi.org/10.1128/IAI.00525-07.
44. **Worth RG, Kim MK, Kindzelskii AL, Petty HR, Schreiber AD.** 2003. Signal sequence within Fc gamma RIIA controls calcium wave propagation patterns: apparent role in phagolysosome fusion. Proc. Natl. Acad. Sci. U. S. A. **100:**4533–4538. http://dx.doi.org/10.1073/pnas.0836650100.
45. **Vieth JA, Kim MK, Glaser D, Stiles K, Schreiber AD, Worth RG.** 2013. FcgammaRIIa requires lipid rafts, but not co-localization into rafts, for effector function. Inflamm. Res. **62:**37–43. http://dx.doi.org/10.1007/s00011-012-0548-1.
46. **Cox J, Mann M.** 2008. MaxQuant enables high peptide identification rates, individualized p.p.b.-range mass accuracies and proteome-wide protein quantification. Nat. Biotechnol. **26:**1367–1372. http://dx.doi.org/10.1038/nbt.1511.
47. **UniProt Consortium.** 2012. Reorganizing the protein space at the Universal Protein Resource (UniProt). Nucleic Acids Res. **40:**D71–D75. http://dx.doi.org/10.1093/nar/gkr981. PubMed.